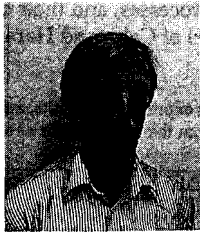


Improved Tests of Muon and Electron Number Conservation In Muon Processes

W. R. MOLZON

Department of Physics and Astronomy, University of California, Irvine, CA 92697-4575



I review the motivation for and status of searches for violation of muon and electron number conservation, concentrating on muon initiated processes. I discuss the expected progress in these searches and describe a new experiment, E940 at BNL, recently proposed by the MECO collaboration and now approved. It will improve the experimental sensitivity for the process $\mu^- N \rightarrow e^- N$ to below 10^{-16} , roughly 4 orders of magnitude better than the current limit.

Introduction

Since the discovery of the muon and the realization that all differences between muons and electrons are attributable solely to the difference in their masses, there has been interest in understanding why more than one *family* of leptons exists and how they are related. The fact that the decay $\mu^+ \rightarrow e^+\gamma$ was not observed led to speculation that each type of lepton carries an approximately conserved quantum number, and hence that there exists more than one type of neutrino. We now know that three families of light leptons exist, and that an additive quantum number associated with each family is conserved to a high degree.

Given limits on neutrino mass and mixing, diagrams with loops containing W bosons and neutrinos do not lead to lepton flavor violation at observable levels. Hence, the discovery of LFV processes would indicate the existence of new physics. The possibility of LFV exists in essentially all extensions to the Standard Model, and we will discuss some of these in a following section. There has been recent progress in LFV searches using both kaon and muon processes. We list in table 1 the LFV processes which have been studied, the current experimental limits on these processes, and their classification in terms of a change in *generation number* (ΔG) in the model of Cahn and Harari¹.

Table 1: LFV violating process, the current experimental limits, and the inferred limits on intermediate particle masses (updated from the reference for new experimental results).

Process	ΔG	BF Limit (90% CL)	Mass Limit (TeV)
$K_L^0 \rightarrow \mu e$ (Ref. ^{2,3})	0,2	2.4×10^{-11}	100
$K_L^0 \rightarrow \pi \mu e$ (Ref. ⁴)	0,2	3.2×10^{-10}	37
$K^+ \rightarrow \pi \mu e$ (Ref. ⁵)	0	2.1×10^{-10}	29
$\mu^+ \rightarrow e^+ e^+ e^-$ (Ref. ⁶)	1	1.0×10^{-12}	86
$\mu^+ \rightarrow e^+ \gamma$ (Ref. ⁷)	1	3.8×10^{-11}	20
$\mu^- N \rightarrow e^- N$ (Ref. ⁸)	1	7.8×10^{-13}	500

In the remainder of this paper, we will briefly discuss physics models which allow lepton flavor violation. We will then give an overview of the experimental techniques involved in $\mu \rightarrow e^+\gamma$ and $\mu^- N \rightarrow e^- N$ experiments, and discuss the experiments which have given the most stringent limits. Finally, we will describe a new experiment which is proposed to improve substantially the search for $\mu^- N \rightarrow e^- N$.

Theoretical Motivation for LFV Searches

Many proposed extensions to the Standard Model allow lepton flavor violation. In general, these models are not devised for the purpose of predicting LFV, and the current stringent LFV limits already restrict the allowed values of model parameters. Feynman diagrams for new processes which could contribute to LFV are shown in figure 1; these are summarized in the literature⁹. In most models, there is no particular scale at which lepton flavor violation should occur, since masses, coupling strengths and mixing angles of new particles are not predicted. Nonetheless, the reach in parameter space of current and proposed experiments is impressive.

Much interest has occurred recently in grand unified supersymmetric models. It was realized, first by Hall and Barbieri, that LFV will occur at experimentally accessible levels in

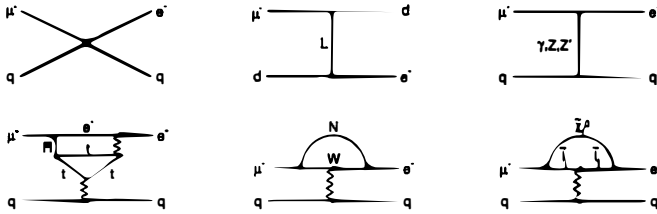


Figure 1: Feynman diagrams for the process $\mu^- N \rightarrow e^- N$ in different scenarios for non Standard Model physics.

a large class of supersymmetric models^{10,11,12,13}. Further, in some specific grand unified supersymmetric models, the rate for LFV processes can be related directly to standard model parameters. If these models are correct, searches for $\mu^- N \rightarrow e^- N$ with sensitivity 10^{-16} or $\mu^+ \rightarrow e^+ \gamma$ with sensitivity 10^{-14} may discover lepton flavor violation. Even if supersymmetric particles are discovered at colliders, the measurement of LFV violating processes will be extremely important in understanding symmetry breaking in the interactions.

Overview of LFV Searches Using Muons

Muon initiated LFV processes have been studied extensively. The most familiar is $\mu^+ \rightarrow e^+ \gamma$ decay; there is an ongoing experiment⁷ and there have been discussions about the possibility of executing experiments with even better sensitivity¹⁴. A second process is $\mu \rightarrow eee$; it is closely related to $\mu^+ \rightarrow e^+ \gamma$ if mediated by a γ . At the same branching fraction it is less sensitive to the underlying physics due to an extra factor of α in the decay rate. The limit is very good⁶ and there are no proposals for new experiments. A third reaction is $\mu^- N \rightarrow e^- N$. If the process is mediated by a photon, the ratio $R_{\mu e} \equiv \Gamma(\mu^- N \rightarrow e^- N) / \Gamma(\mu^- N \rightarrow \nu N')$ is about 300 times smaller¹⁵ than $\tilde{B}(\mu^+ \rightarrow e^+ \gamma)$. There is an ongoing experiment⁸, and a new experiment^{17,18} has been approved.

Ongoing $\mu^+ \rightarrow e^+ \gamma$ Experiments

A search for $\mu^+ \rightarrow e^+ \gamma$ is conceptually simple. A beam of μ^+ is brought to rest in a thin target in which the muons decay. The signature is a photon and an electron, each with energy $\sim m_\mu/2$, originating from a common point and with opposite momenta.

An intrinsic background arises from radiative muon decay when both neutrinos are emitted with approximately zero energy. It is reduced by requiring the measured e^+ and γ momenta to be opposite in direction and sufficiently close to $m_\mu/2$ that the radiative decay background satisfying these requirements is below the desired sensitivity. A second source of background arises from the accidental overlap of two decays, each providing one of the final state particles. Requirements on the time coincidence of the two particles and their intersection at a common origin provide additional background rejection tools. At the stopping intensities required to measure branching fractions below 10^{-12} , the accidental background dominates.

The state of the art is the MEGA experiment⁷ at LAMPF; it completed data taking in 1995. The experiment stopped $\sim 1.5 \times 10^{14}$ stopped muons, and wrote $\sim 5 \times 10^8$ events to tape. Briefly, the detector consisted of a set of proportional wire chambers, drift chambers,

and scintillation counters in a solenoid. The helical trajectory of electrons was measured in drift chambers. Photons were converted in thin radiators and the trajectories of the resulting e^+e^- pairs measured to deduce the photon momentum.

Results of $\sim 16\%$ of the data have been reported⁷; from these data an upper limit $B(\mu^+ \rightarrow e^+\gamma) < 3.8 \times 10^{-11}$ at 90% confidence level was set. Based on full analysis of the data and possible improvements in analysis efficiency, an upper limit of $3 - 6 \times 10^{-12}$ is expected to be set, assuming no events are seen.

There are no proposals for more sensitive searches for this process, although a number of ideas for experiments which could reach a sensitivity close to 10^{-14} have been discussed¹⁴.

Ongoing $\mu^-N \rightarrow e^-N$ Experiments

The sensitivity goals of $\mu^-N \rightarrow e^-N$ searches are more ambitious than those of $\mu^+ \rightarrow e\gamma$ searches, since in a variety of models, $R_{\mu e}$ is ~ 300 times smaller than $B(\mu^+ \rightarrow e\gamma)$. Better sensitivity is possible due to the lack of the kind of accidental backgrounds which limit $\mu^+ \rightarrow e^+\gamma$ experiments.

The experiment is done by bringing μ^- to rest in a thin target; they quickly become Coulomb bound to nuclei, and either decay or are captured (with about equal probability for moderate size nuclei). The signature of coherent $\mu^-N \rightarrow e^-N$ (in which the nucleus is left in its ground state) is an isolated electron originating in the stopping target, with the e^- energy equal to $m_{\mu}c^2$ less a small binding energy and nuclear recoil energy (a total of < 1 MeV). The coherent rate is enhanced by about a factor of Z compared to incoherent processes.

The principal experimental difficulties are getting sufficient μ^- flux and reducing backgrounds due to other sources of 105 MeV electrons. One class of backgrounds is intrinsic, for example μ^- decay in orbit, with the endpoint of the e^- energy distribution equal to the signal energy. These can be reduced only by improved electron energy resolution. A second class results from electron and pion contamination in the beam and from cosmic rays, and these can be reduced or eliminated with beam and detector design. Because there is no inherent accidental background, the stopping rate can be very high.

The state of the art is the SINDRUM2 experiment⁸ at PSI. A limit $R_{\mu e} < 7.8 \times 10^{-13}$ at 90% confidence level has been set. They propose to improve their sensitivity to 4×10^{-14} with a new beam and new background rejection technique. Figure 2 shows a cut view of the apparatus. It is a cylindrical detector, with drift chambers in a solenoid field to measure the e^- momentum. About $10^7 \mu^-/s$ are stopped in a target on the axis of the solenoid. The beam is continuous, and contains a mixture of μ^- , π^- and e^- . Backgrounds from beam contamination are eliminated by rejecting events in which a signal is detected in a thin scintillator in the beam, time coincident with the event. Figure 2 shows the SINDRUM2 data; after all cuts are applied, non-intrinsic backgrounds are eliminated, and the background due to μ decay in the Coulomb bound orbit is well separated from the expected signal.

The SINDRUM2 collaboration proposes to upgrade the beam to eliminate all π^- and high momentum e^- . This will allow them to remove the beam veto and increase the stopping rate to $10^8 s^{-1}$. The beam they propose must reduce π^- and e^- contamination in the beam by a factor of 4000. They have encountered¹⁶ difficulty with the beamline elements, and hope to start taking data later in 1998 with a titanium target, with a goal of reaching a sensitivity below 10^{-13} .

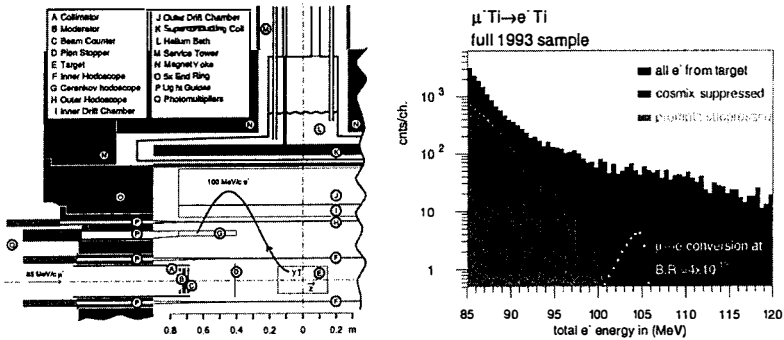


Figure 2: A cut view of the SINDRUM2 $\mu^- N \rightarrow e^- N$ apparatus is shown on the left. The histogram shows detected electron energy distributions; the lightly shaded contribution is after all cuts have been applied and consists primarily of electrons from muon decay in orbit. The medium shaded region contains background removed by vetoing on events which are in time with a signal in the beam counter, and the heavily shaded area contains events removed by cosmic ray cuts.

The MECO $\mu^- N \rightarrow e^- N$ Experiment

The Muon to Electron Conversion collaboration has recently proposed^{17,18} to improve the sensitivity for $\mu^- N \rightarrow e^- N$ to below 10^{-16} using a new beam and detector operating at the Brookhaven National Laboratory (BNL) Alternating Gradient Synchrotron (AGS). Many of the ideas for the basic design of the beam and experimental arrangement are taken from the early work of Lobashev and Djilkibaev^{19,20}. A schematic drawing of the MECO beam-line and experimental area is shown in figure 3.

A critical aspect of MECO is a very intense μ^- beam; it will be the highest intensity muon beam ever produced. MECO proposes²¹ to operate the AGS at ~ 8 GeV/c, with 4×10^{13} protons per pulse, with 50% duty factor and 1 second rep rate. The π^- from which the muons result are produced in a tungsten target located in a graded solenoidal field;

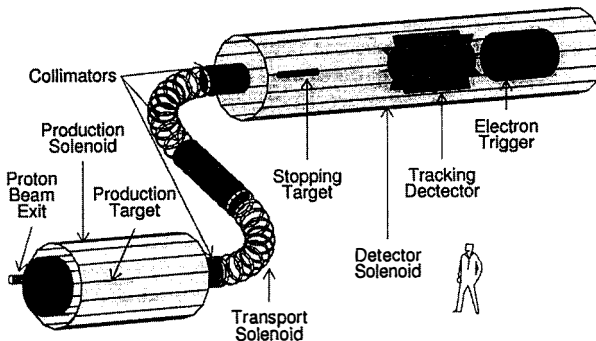


Figure 3: Schematic drawing of the production solenoid, transport solenoid, and detector solenoid with the targets, collimators, and detectors.

π^+ 's are collected over essentially 4π solid angle. The μ^- beam resulting from π^- decays is transported to the stopping target and detector region in a curved transport solenoid. The effect of the curvature on particles propagating in helical trajectories in the solenoid is exploited to sign and momentum select the beam. The flux delivered to the stopping target is $\sim 0.01 \mu^-$ per proton.

A second critical feature of MECO is a pulsed beam to significantly reduce the backgrounds from π^- and e^- contamination in the beam. A pulsed beam was used in an earlier experiment²². The idea is to stop a pulse of μ^- and detect conversion electrons only after all π^- and e^- in the beam have either decayed or passed through the detector region. The pulse spacing must be sufficient to allow all beam particles to disappear and must be comparable to the μ^- lifetime. This leads to a pulse frequency of ~ 1 MHz and the use of an Aluminum stopping target, in which the μ^- lifetime is 880 ns. The extinction (ratio of the number of protons between pulses to that in the pulses) has been shown to be required to be $< 10^{-9}$, in order to reduce background to negligible levels.

The MECO beam will be produced from an appropriately pulsed proton beam, implemented using the RF structure of the AGS. The proposed operation of the AGS is with 2 filled bunches in the $2.7 \mu\text{s}$ revolution time, extracting the beam without de-bunching²¹. Initial tests of a bunched extracted beam were done in 1996, and achieved an extinction of below 10^{-6} . Substantially improved performance is expected²¹ with additional tuning of the AGS operation. It is planned to test operations of the AGS at the full intensity and with the time structure required for MECO during summer 1998. If sufficient extinction cannot be achieved in the extracted beam, a pulsed kicker in the proton transport line is foreseen. Both electrostatic and magnetic devices are being studied.

The MECO muon beam has been simulated extensively. Low energy pion production cross sections have not been measured extensively. Data has been collected by E910²³ at BNL and is now being analysed. Calculations based on a number of hadronic cascade codes vary by a factor of 6. The production and transport parameters were optimized, and the resulting μ^- yield calculated using the GHEISHA²⁴ code in the GEANT simulation package. Subsequent to those calculations, the results of which are contained in the MECO proposal, a measurement²⁵ of low energy pion production by 10 GeV protons on heavy targets was found which indicates the GHEISHA model overestimates the yield by about a factor of two; the sensitivity shown below is based on scaling the yields from the GHEISHA calculation by this factor.

The μ^- stopping target and detector are located in the detector solenoid. Muons are stopped in a thin Aluminum target consisting of 17 layers with a total thickness of 34 mm. The detector is located downstream of the target in order to minimize rates in it due to particles coming from the target. The field is axially graded, starting at 2 T at the entrance and grading to 1 T before the tracking detector. This results in very good acceptance for 105 MeV electrons originating in the target. Electrons emitted at $90^\circ \pm 30^\circ$ with respect to the beam direction are detected with good efficiency. Sample trajectories illustrating this are shown in figure 4. The use of a graded field also allows electrons produced in the upstream pole piece of the production solenoid to be unambiguously distinguished from those produced in the target, since the transverse momentum of these background events is necessarily smaller than that of e^- produced in the stopping target.

The heart of the detector is the magnetic spectrometer in which the e^- momentum is measured. The tracking detector is low mass in order to minimize the contributions of multiple scattering and energy loss to the electron energy resolution. It consists of axial straw detectors, ~ 2 m long, arranged in a cylinder and 8 vanes. The performance of the de-

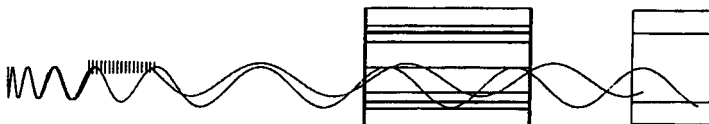


Figure 4: A schematic drawing of the MECO detector region with two typical conversion electron trajectories produced by the GEANT simulation superimposed.

tectors was calculated using a full GEANT simulation of the stopping target and detectors. The intrinsic resolution of the spectrometer has σ_{RMS} of ~ 100 keV, and the total resolution, including energy loss straggling in the stopping target has a FWHM ~ 750 keV.

The electron trigger detector's primary purpose is to select events to be recorded for off-line analysis by requiring a deposited energy consistent with that of a 105 MeV electron. In addition, it provides some confirmation of the e^- energy, aids in distinguishing e^- from other particles, and helps in identifying backgrounds from particles produced by cosmic rays. The proposed detector is a scintillator cylinder approximately 1.2 m long, segmented azimuthally and axially. It is read out by WLS fiber.

The detector region is surrounded by a cosmic ray shield, which minimizes the rate of production of electrons by cosmic ray muons and identifies the e^- that are produced by cosmic rays traversing the detector. It consists of 0.5 m of steel (some of which is provided by the return yoke of the magnet) surrounding the detector solenoid, two layers of plastic scintillator, and 2 m of concrete shielding. The resulting background rate was calculated with a GEANT simulation, using measured CR muon fluxes as input. In a simulation equivalent to ~ 200 years exposure, three events (equivalent to 0.0035 events in 10^7 seconds of running) satisfied all selection criteria.

Physics Background Sources

Physics backgrounds potentially originate from a variety of sources: μ^- decay in a Coulomb bound orbit, radiative μ^- capture, beam electrons, μ^- decay in flight, π^- decay in flight, radiative π^- capture, \bar{p} induced electrons, and cosmic ray induced electrons. The first two are intrinsic to μ^- stopped in the target; they can be minimized only by improving the measurement of the electron energy. The other sources derive from prompt processes, with the electron detected close in time to the arrival of a particle in the detector, and are reduced with a pulsed beam. Very slow \bar{p} 's have a very long transit time in the muon beam-line and arrive at the stopping target essentially continuously. Hence, they are not significantly reduced by using a pulsed beam. Cosmic ray background is reduced with appropriate active and passive shielding.

Potential sources of backgrounds were studied extensively by the MECO collaboration^{17,18}. Particle production, decay, and interaction in the beam and detector were simulated using the GEANT code package. The simulation included effects of scattering in the beam-line and collimators, inhomogeneities in the magnetic field in the transport region, and energy loss throughout the beam-line. Some processes which are not well modeled by GEANT were calculated with a combination of analytic and Monte Carlo techniques. For example, large angle scattering of electrons in the stopping target was simulated using the Mott scattering formula with nuclear form factors. Rates for some processes (radiative π^- and μ^- capture for example) have been taken from the literature and incorporated in a

Monte Carlo calculation of the background.

The largest source of background is that due to μ^- decay in orbit and this background source drives the design of the detector. The energy distribution is approximately proportional to $(E_{max} - E_e)^5$ near the endpoint²⁷. Hence it is extremely sensitive to both the central

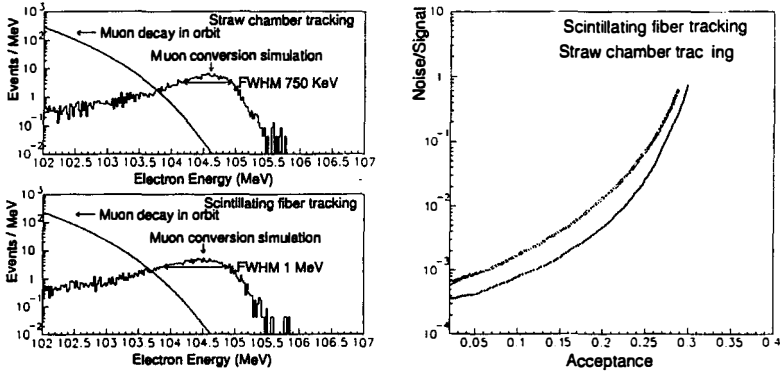


Figure 5: The histograms on the left show simulations of the expected signal and background for $R_{\mu e} = 10^{-16}$ for two detectors. The normalization of the curves is for $R_{\mu e} = 10^{-16}$ and a luminosity corresponding to 10^7 seconds running time. On the right is a parametric plot of the background/signal and acceptance as a function of the minimum allowed measured e^- energy.

part of the detector response function and possible high energy tails. Figure 5 shows the signal and background for $R_{\mu e} = 10^{-16}$, calculated in a full GEANT simulation. By accepting events between 103.9 MeV and 105.4 MeV, the noise to signal ratio is below 0.05 and the signal acceptance is large.

Potential background from $\bar{\nu}$'s and their annihilation products has been studied recently. A thin beryllium window in the muon transport channel absorbs all produced $\bar{\nu}$. The resulting contribution to the background from the resulting π^- and e^- annihilation products was calculated by Monte Carlo simulation.

Backgrounds from all sources are summarized in the next section.

Expected Performance and Sensitivity of MECO

The sensitivity which will be achieved by MECO is summarized in table 2. In 10^7 s running time, a few events can be detected at a value of $R_{\mu e} = 10^{-16}$.

Table 3 shows the expected background rates for the sensitivity quoted above. It is dominated by the μ^- decay in orbit contribution. Substantial improvement in discrimination against this source of background can be had with modest loss in acceptance, as shown in figure 5. A proton beam extinction of 10^{-10} is assumed, and backgrounds from all but the first two sources scale with this extinction.

Summary

Experiments to search for violation of muon and electron number have now been done for over 40 years, with ever increasing sensitivity. Current limits on muon induced processes

Table 2: A summary of the expected MECO sensitivity for a one year (10^7 s) run.

Running time (sec)	10^7
Proton flux (sec^{-1})	4×10^{13}
μ/p entering solenoid	0.006
Stopping probability	0.370
μ capture probability	0.600
Fraction of μ which capture in time window	0.480
Electron trigger efficiency	0.900
Fitting and selection criteria	0.250
Detected events for $R_{\mu e} = 10^{-16}$	5.800

Table 3: A summary of the level of background from various sources calculated for a sensitivity of ~ 5 events for $R_{\mu e} = 10^{-16}$.

Source	Events	Comment
μ decay in orbit	0.290	$S/N = 20$ for $R_{\mu e} = 10^{-16}$
Radiative μ capture	$\ll 0.050$	
* μ decay in flight	< 0.003	without scatter in target
* μ decay in flight	0.004	with scatter in target
* Radiative π capture	0.007	from out of time protons
Radiative π capture	0.004	from late arriving π
* π decay in flight	$\ll 0.001$	
* Beam electrons	< 0.002	
\bar{p} induced	0.004	mostly from π^-
Cosmic ray induced	0.004	10^{-4} CR veto inefficiency
Total background	0.370	* assumes 10^{-10} extinction

are at the level of 10^{-11} to 10^{-12} for the processes $\mu^+ \rightarrow e^+\gamma$, $\mu^+ \rightarrow e^+e^+e^-$, and $\mu^-N \rightarrow e^-N$. These limits place stringent constraints on many scenarios for physics beyond the Standard Model.

Improvements in muon beams and detector technology hold promise for making further significant improvements in the sensitivity of searches in the next few years. In particular, the SINDRUM2 experiment being done at the PSI laboratory is expected to improve the sensitivity to $\mu^-N \rightarrow e^-N$ to below 10^{-13} in the next year or two. Further improvement, to a sensitivity below 10^{-16} , is promised by the MECO experiment, now approved at BNL. Ideas have been discussed for improving the sensitivity to $\mu^+ \rightarrow e^+\gamma$ to near 10^{-14} . If these proposed experiments are successfully executed, they will be sensitive to the level of lepton flavor violating signals suggested in many models. In particular, predictions of a class of grand unified supersymmetric models will be confronted directly by experimental measurements. The very substantial expected improvement in experimental sensitivity, coupled with the predictions of grand unified supersymmetric models, allow some optimism that the first evidence for muon and electron number violation may be found.

References

1. R. Cahn and H. Harari *et al.*, Nucl. Phys. B 176, 135 (1980).

2. K. Arisaka, *et al.*, Phys. Rev. Lett. **70**, 1049 (1993).
3. T. Akagi, *et al.*, Phys. Rev. Lett. **67**, 2614 (1991).
4. P. Krolak *et al.*, Phys. Lett. B **320**, 407 (1994).
5. A. M. Lee *et al.*, Phys. Rev. Lett. **64**, 165 (1990).
6. U. Bellgardt *et al.*, Nucl. Phys. B **299**, 1 (1988).
7. M.D. Cooper *et al.*, *Proceedings of Sixth Conference on the Intersections of Particle and Nuclear Physics*, edited by T.W. Donnelly, (ALP Conference Proceedings 412, 1997), pp 34-48.
8. F. Riepenhausen, presented at the *Sixth Conference on the Intersections of Particle and Nuclear Physics*, Big Sky, Montana (1997).
9. W. Marciano, *Proceedings of the 4th KEK Topical Conference on Flavor Physics*, edited by Y. Kuno and M. Nojiri, Nucl. Phys. B **59** (1997).
10. Barbieri, *et al.*, "Violations of Lepton Flavor and CP in Supersymmetric Unified Theories", IFUP-TH 72/94, January 1995;
R. Barbieri, L. Hall, and A. Strumia, Nucl. Phys. B **445**, 219 (1995).
11. Arkani-Hamed, *et al.*, "Flavor Mixing Signals for Realistic Supersymmetric Unification", LBL-37343 (1996).
12. Barbieri and Hall, "A Grand Unified Supersymmetric Theory of Flavor", LBL-38381 (1996).
13. Hisano *et al.*, "Exact Event Rates of Lepton Flavor Violating Processes in Supersymmetric SU(5) Model", LBL-38653 (1996).
14. Y. Kuno and Y. Okada, LANL hep-ph/9604296 (1996);
Y. Kuno, A. Maki and Y. Okada, LANL hep-ph/9609307 (1996); C. Walter, private communication.
15. A. Czarnecki, W. Marciano and K. Melnikov, hep-ph/9801218 (1997).
16. A. van der Schaaf, private communication.
17. M. Bachman, *et al.*, "A Search for $\mu^- N \rightarrow e^- N$ with Sensitivity Below 10^{-16} ", AGS P940 (1997).
18. Numerous internal MECO documents can be found in the WWW server <http://meco.ps.uci.edu/>.
19. R.M. Djilkibaev and V.M. Lobashev, Sov. J. Nucl. Phys. **49(2)**, 384 (1989).
20. V.S. Abadjev, *et al.*, "MELC Experiment to Search for the $\mu^- A \rightarrow e^- A$ Process", INR preprint 786/92, November 1992.
21. M. Brennan, private communication.
22. Badert *et al.*, Nucl. Phys. A **377**, 406 (1979).
23. I. Chemakin *et al.*, P910 to BNL AGS (1995).
24. H.C. Fesefeldt, "Simulation of Hadronic Showers, Physics and Applications", PITHIA Report, Aachen 85-02 (1985).
25. D. Artnutliski, *et al.*, Sov. J. Nucl. Phys. **48**, 161 (1988).
26. O. Allkofer, *et al.*, Nucl. Phys. B **259**, 1 (1971).
27. O. Shankar, Phys. Rev. D **25**, 1847 (1982).